



## Research Article

## Acoustic, Mechanical and Thermal Properties of Luffa/Jute Fiber-Reinforced Bio-Composites

Johnson Annie Suba\*

Assistant Professor, Department of Costume Design and Fashion, Bishop Appasamy College of Arts and Science, Coimbatore, Tamil Nadu, India

Senthil Kumar Boominathan

Assistant Professor, Department of Rural Industries and Management, The Gandhigram Rural Institute (DU), Gandhigram, Tamil Nadu, India

\* Corresponding author. E-mail: jasuba75@gmail.com DOI: 10.14416/j.asep.2024.08.006

Received: 14 April 2024; Revised: 13 June 2024; Accepted: 24 July 2024; Published online: 16 August 2024

© 2024 King Mongkut's University of Technology North Bangkok. All Rights Reserved.

### Abstract

Due to the growing environmental awareness, more attention has been drawn to finding alternative fiber sources to curb deforestation and reduce the usage of synthetic fiber. In the current work, an attempt was made to hybrid bio-composites using the blended fibers of Luffa and Jute in different ratios. Eight different needle-punched nonwoven fabric samples were prepared with the variation of fiber blend ratios. Both the fibers were pre-treated with a 3% alkali concentration to enhance the bonding property with the resin. After this process, the polymer composites were produced using epoxy resin through the compression molding technique. The investigations, such as physical, mechanical, water absorption, dynamic mechanical (DMA), and acoustic properties of the composite material were analyzed systematically. The mechanical and DMA properties were appreciable for composites with higher jute content, whereas acoustic properties were higher for composites with higher Luffa content. Based on the findings, the hybrid composites showed effective functional performance in load-bearing and acoustic applications.

**Keywords:** Biomaterials, Luffa composites, Luffa fibers, Porous materials, Sound absorption, Transmission loss

### 1 Introduction

Due to environmental awareness, natural fiber development is essential, and its utilization has recently drawn more attention towards the material science sector [1], [2]. Moreover, natural fibers are relatively inexpensive, biodegradable, have higher mechanical loading resistance and thermal resistance, and are sustainable. Due to their fibrous structure and large total surface area, fiber-based nonwoven materials are perfect for applications requiring sound insulation and sound absorption [3], [4]. Many investigations have been done on natural fiber-based materials for acoustic applications.

Lee and Joo studied the recycled polyester nonwovens as a sound absorber. The nonwoven absorber with the intermediate layer of nonoriented web exhibited a more significant noise absorption

coefficient (NAC) than those with web structures that were oriented [5]. Kuncoro *et al.*, combined *Ceiba petandra* fiber reinforced composite with metal-based fillers and snail powder to increase the thermal resistance of natural fiber composite. The fillers have significantly, they discovered. They found that the fillers have substantially improved the thermal properties of the composites [6]. Femiana *et al.*, enhanced the tensile strength of the composite by 155.72 Mpa when combining timoho fiber with iron powder interfaced through polyester resin composite. Additionally, thermal stability and flame resistance were also improved [7]. Andoko *et al.*, fabricated a hybrid composite with *Ceiba petandra* fiber and carbon fiber to produce ideal mechanical performance [8]. Tascan and Vaughn investigated the effect of the fiber profile surface of needle-punched nonwoven fabric on the acoustic properties of the composite. It

was reported that the polyester fiber with octobal and trilobal cross sections has shown higher sound absorption capacity and fiber fineness, which also influences the acoustic properties of the material [3]. Kucuk and Korkaz investigated the influence of fiber blending on the acoustic properties of the nonwoven material. It was found that the cotton/PET blend with a 70%: 30% ratio has shown higher sound absorption properties than other combinations [9]. According to Zent *et al.*, blended fiber-based nonwoven structures outperform single fiber-based nonwoven materials in terms of noise reduction [10]. Additionally, the nonwoven's internal pore structure plays a significant role in deciding the acoustic properties of the material, for example greater number of pores will result in a greater source absorption property [11]. The Luffa fibers, one of the novel vegetable fibers can be utilized in household appliances, automobiles, and architectural applications [12]. A lot of research has been done on the mechanical properties of Luffa fiber-based materials, and this research discusses the composite structures of Luffa blended with Jute fiber. More specifically, this discussion is about the mechanical and acoustic properties of blended fiber composites.

## 2 Materials and Methods

The two different natural fibers utilized for nonwoven reinforced composite production are Jute and Luffa. This Jute fiber was sourced from the market, whereas the Luffa fiber was extracted from the dried shell of *Luffa aegyptiaca* vegetable. The collected fibers were scoured with 3% NaOH to remove the natural impurities such as wax, and hemicelluloses and to improve the crystallinity of the fiber. The physical properties of the fibers are shown in Table 1, and the images of the fibers are shown in Figure 1.

**Table 1:** Physical properties of Luffa and jute Fibers.

Properties	Luffa Fiber	Jute Fiber
Fiber length(cm)	5.76	8.28
Fiber Diameter( $\mu\text{m}$ )	$36 \pm 0.5$	$33 \pm 0.6$
Density (g/cc)	1.12	1.23
Tensile strength (Mpa)	86.7	142
Average Modulus (Gpa)	1.05	1.12
Elongation (%)	1.12	1.3
Moisture content	7.8%	10.06%

### 2.1 Nonwoven making

The separated fibers were cut into two different dimensions such as 5–6 cm for Luffa fiber and 8–8.5 cm for Jute fiber. Both fibers were blended with six different combinations as per Table 2 for needle-

punched nonwoven fabric production. Previously, the tabletop carding machine was utilized for opening, cleaning and producing the parallel-laid carding web. This parallel-laid web was presented to the needle punching machine. This needle punching process was carried out through a Dilo needle punching machine with a punching density of 29 inches/sq.cm, a punching depth of 15 mm, and a needle punching frequency of 250 strokes per minute.

#### 2.1.1 Resin bonded composite making

To analyze the influence of different fiber mixing on the functional properties, the fiber volume percentage was kept at 65% for all the samples during the composite Making. A  $150 \times 150 \times 5$  mm mold was utilized to fabricate the composite. The epoxy resin (CY225 with HY225 hardener) was injected into the mold cavity. To create the compact composite structure 35% equivalent volume of resin was put into each nonwoven fabric layer. The mold unit was then transferred to the compression molding machine after finishing the laying phase. 30 bar of pressure was applied to the mold via the compression molding machine. Figure 1 depicts a composite specimen and the fabrication process for composites. The composite sample images are shown in Figure 2.

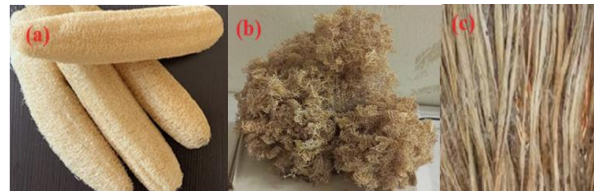


**Figure 1:** Fibers used for nonwoven production; (a) Luffa Fiber assembly, (b) Chopped Luffa Fiber, and (c) Jute Fiber.

## 2.2 Characterization

### 2.2.1 Physical properties

The porosity of the nonwoven is the ratio between the density of the nonwoven to the density of the fiber. The measured densities of the luffa and jute fiber were  $1.12\text{g/cm}^3$  and  $1.23\text{g/cm}^3$ , and the nonwoven density was measured through the weighing balance method.

$$A = \frac{\rho_{\text{fabric}}}{\rho_{\text{fiber}}} \times 100$$

$$\text{Porosity \%} = (1 - A)^2$$

**Table 2:** Nonwoven specifications made with different fibre blending ratios.

Sample No.	Fiber Mixing Ratio	Average Thickness	Bulk Density (g/m <sup>2</sup> )	Porosity %	Weight (g/sq.m)	Calculated Porosity %	Air permeability (Cm <sup>3</sup> /Cm <sup>2</sup> /s)
N1	35 % Luffa/ 65 % Jute	1.4 mm	24.23	99.8	82.13	83.23	30.23
N2	45 % Luffa/ 55 % Jute	1.65 mm	22.45	99.81	80.64	84.02	34.23
N3	50 % Luffa/ 50 % Jute	1.75 mm	21.34	99.82	79.20	84.43	38.42
N4	65 % Luffa/ 35 % Jute	2 mm	18.42	99.84	73.25	85.68	40.34
N5	75 % Luffa/ 25 % Jute	1.84 mm	18.21	99.84	72.45	86.51	45.32
N6	85 % Luffa/ 15 % Jute	2.5 mm	17.56	99.85	70.24	87.37	48.23

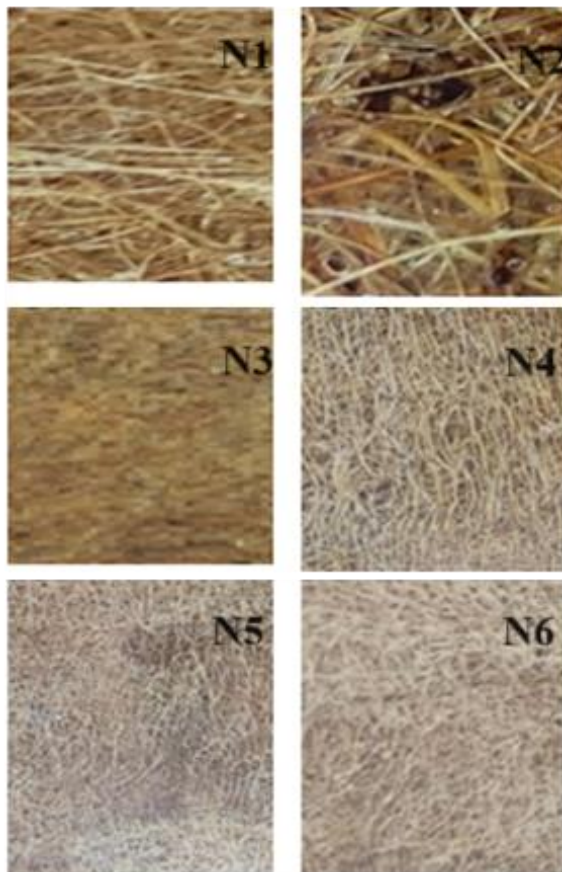


**Figure 2:** Composite samples made with different reinforcement ratios (N1–N6). As per ASTM Test Method D 737, the Air permeability of the nonwoven fabrics was measured. It is the measure of air flowing perpendicular to the known area of the nonwoven material, and it is indicated in the form of cm<sup>3</sup>/cm<sup>2</sup>/s. Areal density, bulk density and porosity of the nonwoven fabric samples were included in Table 2.

### 2.2.2 FTIR

The chemical composition present in Luffa fiber and the influence of alkali pre-treatment on luffa fiber was ascertained through FTIR spectroscopy. A Jasco FT/IR-6300 type A spectrometer was utilized to assess the same. The spectrum was recorded between 5000 cm<sup>-1</sup> to 500 cm<sup>-1</sup>.

### 2.2.3 Mechanical testing

Instron's Zwick Roell-Z010 Universal Testing equipment was used to test the composite samples' tensile, flexural, impact, and Rockwell hardness in accordance with ASTM D3039M, ASTM D790, ASTM D3410, and ASTM D2240, respectively. The rate of loading for tensile and flexural testing was kept at 2 mm/min and 2.8 mm/min, respectively. Before the physical tests, nonwoven samples were preconditioned in typical atmospheric circumstances (20±2 °C temperature, 65±5% relative humidity). Five measurements of each sample were taken for the mechanical testing process. Similarly, the composite harness was analyzed with Rockwell Hardness Tester as per ASTM D785-98 standard.

### 2.2.4 Dynamic Mechanical Analysis (DMA)

According to ASTM D 7028-07e1 standard, DMA analysis was carried out using a Netzsch DMA tester. The two parameters, such as storage modulus and loss modulus were analyzed. This is the measure of the visco-elastic property of the composite under different temperature ranges. The experiment was carried out in tensile mode with heating rates of 2 °C/min and 1 Hz starting at 30 °C and going up to 100 °C.

### 2.2.5 Water absorption properties

The specimens' water absorption rate was determined using the ASTM D 570-98 standard. The samples were maintained at 50 °C for 24 h before being cooled in desiccators. At 23 °C, the specimens were submerged in distilled water. The specimens were removed from the water after 24 h, washed off with dry cotton, and weighed. The weight change due to water absorption was calculated as a percentage. The saline water absorption test was performed in the same manner, and the percentage of weight change was calculated.

### 2.2.6 Sound Absorption Coefficient (SAC)

The sound absorption coefficient (SAC) was measured using an impedance tube following ASTM E 1050. One end of the tube is mounted with the test material (bonded nonwoven), and the other end has a facility for creating sound sources. A 100 mm diameter impedance tube measures frequencies from 50Hz to 1.6 KHz. The samples are attached to one end of the tube, and stationary sound waves with the specified frequency are created through the other end of the tube. The sound wave entered the impedance tube, traveled there, hit the sample, and then reflected. The sound pressure is monitored in two fixed points on the tube using a digital frequency analyzer. This sound pressure measurement can be used to determine the sound absorption coefficient. The equation below is used to compute the sound absorption coefficient.

$$\alpha = \frac{I_i}{I_r}$$

$$\alpha = \frac{|P_i|^2 - |P_r|^2}{|P_i|^2}$$

Where  $\alpha$  is the sound absorption coefficient,  $I_i$  is the intensity of the incident sound wave  $I_r$  is the intensity of the reflected sound wave, and  $P_i$  &  $P_r$  denotes the pressure of incident and reflected waves, respectively.

## 3 Results and Discussion

### 3.1 Detection of functional groups

FTIR spectroscopy of untreated and alkali treated Luffa fiber was investigated (Figure 2(a) and (b)).

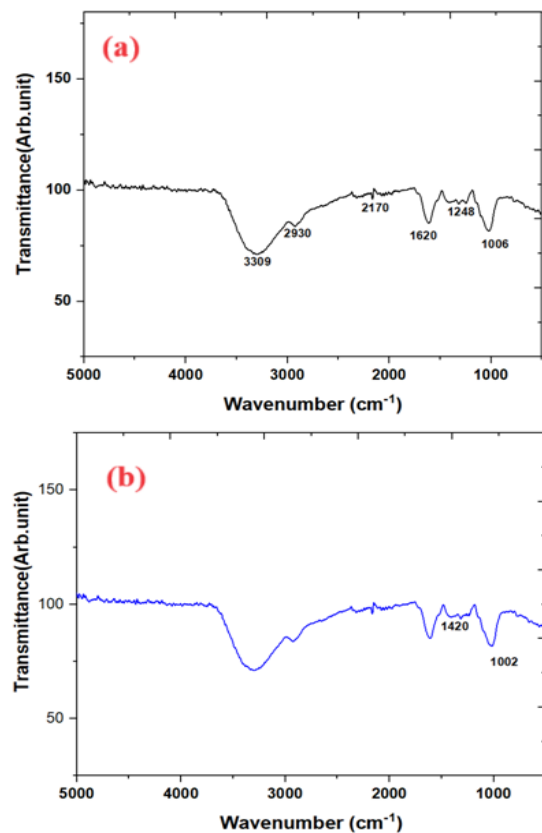


**Figure 2:** FTIR spectra of extracted Luffa fiber; (a) raw fiber and (b) alkali treated fiber.

The raw FTIR spectra of luffa fibre contains the following spectra peaks. The peak at 3009 cm<sup>-1</sup> may be interpreted as the existence of the acid group in cellulose [13]. A peak at 2930 cm<sup>-1</sup> belongs to CH stretching. The peaks at 2170 cm<sup>-1</sup> and 1620 cm<sup>-1</sup> belong to OH stretching in cellulose structure and 1248 cm<sup>-1</sup> shows the presence of hemicellulose. In the alkali treated sample, the peaks at 3009 cm<sup>-1</sup> and 2930 cm<sup>-1</sup> were present, which are interpreted as the presence of cellulose structure and the peak at 1248 cm<sup>-1</sup> was missing since the removal of lignin content due to alkali treatment [14]. This alkali treated fiber would improve the functional group on its surface due to which the bond between the resin and fiber was improved.

### 3.2 Tensile properties

The tensile properties such as maximum tensile load, stress, strain, modulus, and extension % of the composite materials were analyzed and reported in Table 3.

Sample N1 has higher tensile properties such as tensile load (N) of 1894.3 N, extension of 0.945 mm, Stress of 28.12 Mpa, strain of 1.45%, and modulus of 1.84 Gpa. On the other hand, the N6 sample has shown the lowest tensile properties such as tensile load (N) is 913.8 N, extension of 1.123%, Stress of 16.56 Mpa, strain of 2.34%, and modulus of 1.12 Gpa. This kind of trend is due to the percentage of fiber contribution of jute fiber. In all the cases, the Jute fiber content increases, and its tensile properties have also been increased. Increasing the Jute fiber content

improved the stiffness and strength of the composite [15]. Further, the tensile properties of Luffa fiber were inferior to that of Jute fiber, which tends to create more voids in the side structure [16], [17]. In this case, the percentage of Luffa fiber diminishes the tensile strength of the composite by increasing the porosity of the composite materials [18]. Further, by effectively allowing the resin to infiltrate via the reinforcing gaps, the N1 sample's optimized fiber mixing boosted the interlaminar shear strength [19].

**Table 3:** Tensile properties of the composite samples.

Sample	Tensile Load (N)	Extension at Maximum Tensile Load (mm)	Tensile Stress at Maximum Tensile Load (MPa)	Tensile strain at Maximum Tensile load (%)	Modulus (Automatic Young's) (GPa)	SD Value of Modulus
N1	1894.3	0.945	28.12	1.45	1.843	0.245
N2	1634.01	0.934	24.15	1.98	1.754	0.231
N3	1201.37	0.924	20.17	1.84	1.645	0.263
N4	1121.5	1.023	18.23	2.01	1.543	0.253
N5	1012.9	1.123	17.34	2.27	1.276	0.203
N6	913.84	1.123	16.56	2.34	1.123	0.212

**Table 4:** Flexural properties of the composite samples.

Sample	Flexure Load (N)	Flexural Extension at Maximum Flexural load (mm)	Flexural Stress at Maximum Flexure Load (MPa)	Flexural strain at Maximum Flexure load (%)	Modulus (GPa)	SD Value of Modulus
N1	67.23	1.943	46.88	1.95	3.453	0.321
N2	62.32	1.864	43.12	1.86	3.023	0.324
N3	58.34	1.834	41.02	1.86	2.862	0.293
N4	57.31	1.745	39.16	1.93	2.541	0.402
N5	44.23	1.684	34.55	1.86	2.343	0.411
N6	42.84	1.567	31.88	1.78	2.351	0.232

### 3.3 Flexural properties

The flexural properties such as maximum flexural load, flexural stress, strain, modulus, and extension % were analyzed and reported in Table 4.

Sample N1 shows the highest flexural properties such as flexural load (N) of 67.23 N, extension of 1.94%, Stress of 46.88 Mpa, strain of 1.95%, and modulus of 3.45 Gpa. On the other hand, the N6 sample has shown the lowest flexural properties such as tensile load (N) of 42.84 N, extension of 1.567%, Stress of 31.886 Mpa, strain of 1.78%, and modulus of 2.35 Gpa. This kind of trend is due to the percentage of fiber contribution of jute fiber. In all the cases, the Jute fiber content increases, and its flexural properties have also been increased. Increasing the Jute fiber content improved the stiffness and strength of the composite. Further, the flexural properties of Luffa fiber were inferior to Jute fiber, which tends to create more voids in the side structure.

### 3.3 IZOD impact strength

Additionally, examined and shown in Table 5 is the composite samples' impact property (J/m). The sample N1's impact strength of 123.7 J/m was found to be the greatest. Furthermore, sample N6 had the lowest impact strength measurement at 84.22 J/m.

**Table 5:** Impact strength of the composite samples.

Sample	Avg. Impact Strength (J/m)	SD Value of Impact Strength
N1	123.9	4.23
N2	100.15	3.43
N3	82.02	2.43
N4	92.74	3.02
N5	90.21	3.45
N6	84.22	3.61

### 3.4 Hardness

Generally, the fiber matrix dispersion will affect the hardness of the composite structure [20]. Since the selected composite materials belong to the blended



category, the inter-fiber property would affect the hardness of the composite to a larger extent. The tested hardness values of all the composite structures are shown in Figure 3. In all the cases, as the percentage of Luffa fiber increased, the hardness values were reduced significantly. At the same time, samples N3 and N4 have not shown any differences. It is inferred that due to the higher amount of fiber agglomeration, the changes in the hardness values are not obvious.

### 3.5 DMA

The DMA analysis was measured to understand the stiffness or the visco-elastic properties of polymeric composite material. The two different indices of DMA have been analyzed for all the composite specimens such as storage modulus and loss modulus. The details are represented in Figures 4 and 5.

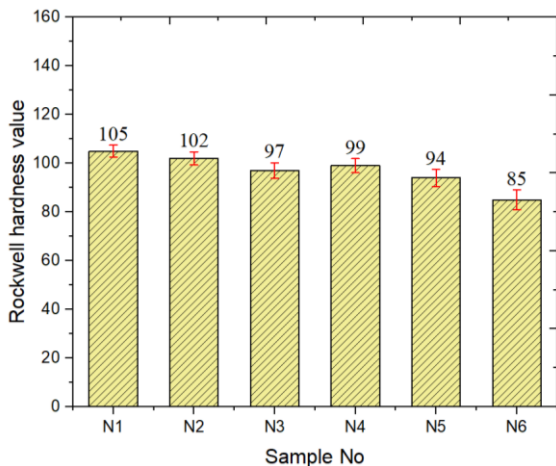


**Figure 3:** The hardness value of the composite material.

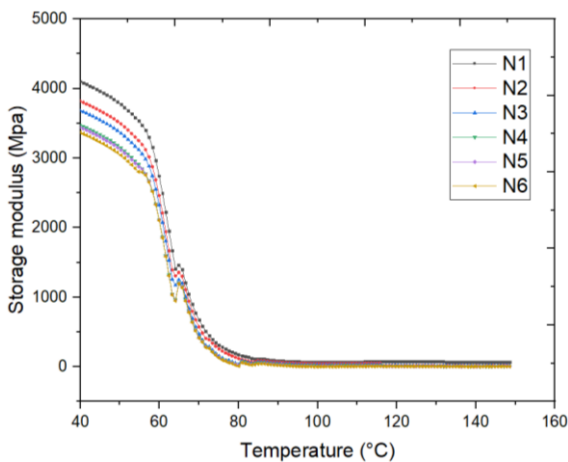


**Figure 4:** Storage modulus of the composite material.

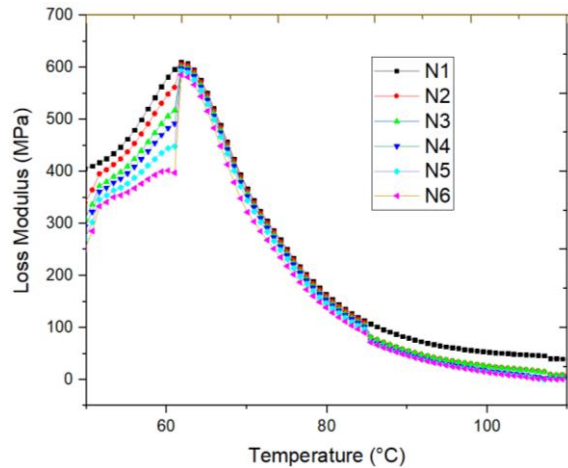


**Figure 5:** Loss modulus of the composite material.

#### 3.5.1 Storage modulus

It is merely the amount of energy absorbed by the composite samples as a result of the cyclic load at various temperatures. The storage modulus of all the composite samples is depicted from 0 °C to 120 °C with 1 Hz frequency. In a general trend, while temperature increases, the storage modulus value decreases. This trend was interpreted as the amorphous phase (resin compound) of the composite attained the relaxation stage. When the jute compound of the composite increases the storage modulus value has increased. This trend was found in the N1 to N6 composite samples. It was interpreted that the modulus of the Luffa fiber is comparatively lesser than that of jute fiber, and the extent of the fiber length is comparatively lesser than that of the jute fiber. The highest storage modulus was obtained for the N1 sample due to its very high level of jute fiber contribution. In this temperature regain, the maximum yield value of N1 composite was attained up to 31155Mpa. The storage modulus increased up to 40 °C, due to an increase in molecular mobility and once it reached its glass transition temperature, the storage modulus started decreasing.

#### 3.5.2 Loss modulus

The measure of energy lost as heat per cycle of deformation is known as the loss modulus ( $E''$ ), and it is the viscous part of the composite material. Figure 5 shows the results of a measurement of the viscous modulus between 20 °C and 100 °C at a frequency of 1 Hz. According to the figure, all Loss modulus was decreased as the temperature increased. As per the

previous cases, the loss modulus increases with the increase in jute fiber composition.

It is interpreted that since both the surrounding polymer and the fiber are elastic by nature, the optimized fiber properties increase energy absorption and so result in a greater loss modulus. In this case, the N1 sample showed the highest loss modulus compared to other samples. It was also discovered that all composite specimens reached the highest loss modulus value in the glassy zone before falling to the lowest range in the temperature range of 60 to 70 °C. When temperature increases, the loss modulus also increases up to 600 Mpa, later, it decreases as a function of temperature. The loss modulus is shown to increase with temperature, indicating a transition from a glassy to a viscoelastic state, and it is the measure of the composite's ability to absorb energy. It also depends upon the friction between the fiber and resin.

### 3.6 Water absorption properties

The water absorption properties of all the test samples were measured with distilled water against different immersion times, and it is graphically represented in Figure 6. In general, the increase of Luffa fiber proportion reduces the water absorption percentage of the nonwoven sample since the comparative moisture regain of Luffa fiber is lesser than Jute fiber. According to the previous researcher, natural fiber composites are generally poor in their water absorption properties [21], [22]. Further to this, the fiber volume percentage also significantly influences the water-holding capacity of the bio-fiber composite structures. According to the above justification, the rest of the samples resembled the ones described above. More specifically N1 sample contains 65% Jute fiber and holds higher moisture intake against various immersion periods due to a higher Jute fiber composition, whereas the N6 sample reflects lesser water holding due to its lesser Jute fiber composition (15%). This condition is reflected in all the test samples. In addition, the cellulose percentage of Luffa fiber is lesser (<60%) than Jute fiber (up to 75%) [23]. Generally, as the cellulose percentage of the fiber increases, the hydrophilic group's presence will proportionally increase, and vice versa. This theory also influenced the improvement of the water absorption percentage of the N1 sample compared to the N6 sample.

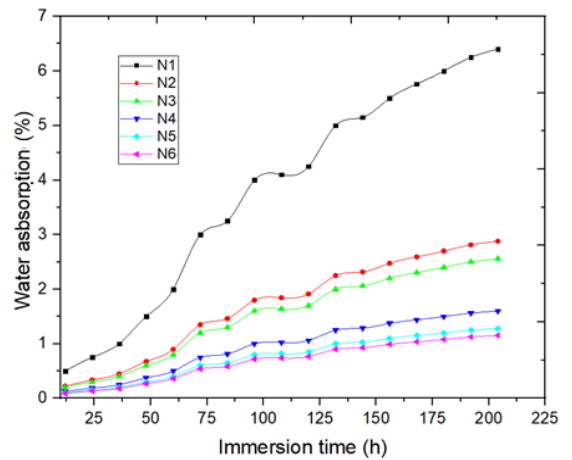


Figure 6: Water absorption properties of the composite material

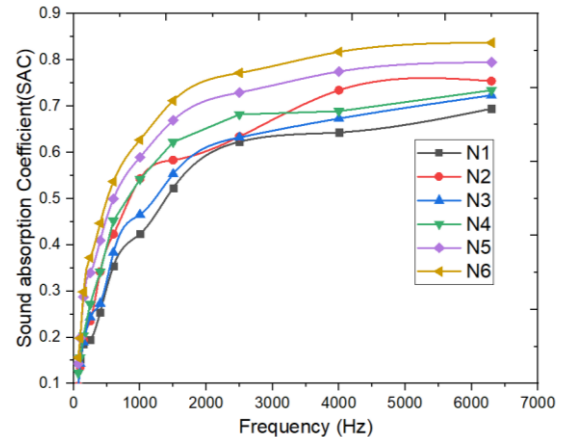


Figure 7: Sound absorption properties of the composite material

### 3.7 Sound Absorption Coefficient (SAC)

The sound absorption coefficient (SAC) value measured through an impedance tube against the frequency range between 0 to 7000 Hz is graphically depicted in Figure 7.

It is preferred that the SAC values of all the samples against low frequencies were low, which is inferred that the low-thickness material with high porosity makes it difficult to block the low-frequency sound waves [24]. This finding again reconfirms this scenario. Subsequently, a gradual increase in sound absorption was found in all the samples. The SAC values at 6300 Hz were found for samples N1 to N6, which are 0.694, 0.754, 0.723, 0.7343, 0.797, and 0.837, respectively. It was also found that fiber blending has



influenced the SAC values significantly. In this investigation as the Luffa fiber proportion increases, SAC values also increase. This is due to the fact that the sound energy penetrates the test specimen and is re-transmitted, which would be measured as the sound absorption coefficient. In this research work, the influence of Luffa fiber created a higher quantum of non-connected structural pores, which would reduce the sound energy significantly [25]–[28]. The highest SAC value was obtained with the N6 sample, which possessed 85% more Luffa samples than other cases. This sustainable Luffa based composite structure can be utilized as a replacement for synthetic acoustic material.

#### 4 Conclusions

In this investigation, the influence of fiber blending on the acoustic and mechanical properties of the composite was studied. Jute and Luffa fiber are the two natural fibers used in this investigation. The needle-punched nonwoven fabric was produced with six different combinations. The fiber blends with 35 % Luffa and 65 % Jute mixing ratio (N1) showed higher values in all the mechanical properties. The tensile and flexural properties of the N1 sample were 28.12 Mpa, and 46.88 Mpa, respectively. DMA studies, such as storage modulus and loss modulus, were analyzed for all the samples. It was found that the N1 sample showed higher performance. Similarly, the impact properties of the N1 sample are 123.7 J/m. In terms of water absorption properties, the N1 sample rated higher due to its higher Jute fiber content than Luffa fiber. On the other hand, the Luffa fiber combination increased the acoustic property of the composite due to its crimp nature. Through this investigation, the Luff blended jute fiber composite can be utilized as a sustainable composite structure that can be utilized for functional applications, including dynamic load bearing and acoustics.

#### Author Contributions

All authors contributed to the study conception and design; J.A.S.: material preparation, data collection investigation, methodology, writing an original draft, editing; S.K.B.: Investigation, analysis, reviewing, editing; All authors have read and agreed to the published version of the manuscript.

#### Conflicts of Interest

The authors declare no conflict of interest.

#### References

- [1] M. Ali, A. Liu, H. Sou, and N. Chow, "Mechanical and dynamic properties of coconut fibre reinforced concrete," *Construction and Building Materials*, vol. 30, pp. 814–825, 2012, doi: 10.1016/j.conbuildmat.2011.12.068.
- [2] R. Phiri, S. M. Rangappa, S. Siengchin, and D. Marinkovic "Agro-waste natural fiber sample preparation techniques for bio-composites development: methodological insights," *Facta Universitatis, Series: Mechanical Engineering*, vol. 21, pp. 631–656, 2023, doi: 10.22190/FUME230905046P.
- [3] M. Tascan, E. and A. Vaughn, "Effects of total surface area and fabric density on the acoustical behavior of needle punched nonwoven fabrics," *Textile Research Journal*, vol. 78, pp. 289–296, 2008, doi: 10.1177/0040517507084283.
- [4] F. Gapsari, L. Djakfar, R. P. Handajani, Y. A. Yusran, S. Hidayatullah, Suteja, S. M. Rangappa, and S. Siengchin, "The application of timoho fiber coating to improve the composite performance," *Results in Engineering*, vol. 15, 2022, Art. no. 100499, doi:10.1016/J.RINENG.2022.100499.
- [5] Y. Lee and C. Joo, "Sound absorption properties of recycled polyester fibrous assembly absorbers," *Autex Research Journal*, vol. 3, no. 2, pp. 78–84, 2003.
- [6] K. Diharjo, F. Gapsari, A. Andoko, M. N. Wijaya, S. M. Rangappa, and S. Siengchin "Flammability and thermal resistance of *Ceiba petandra* fiber-reinforced composite with snail powder filler," *Polymer Composite*, vol. 45, pp. 4947–4960, 2024, doi:10.1002/PC.28100.
- [7] F. Gapsari, A. Purnowidodo, P. H. Setyarini, S. Suteja, Z. Abidin, S. M. Rangappa, and S. Siengchin, "Flammability and mechanical properties of Timoho fiber-reinforced polyester composite combined with iron powder filler," *Journal of Material Research and Technology*, vol. 21, pp. 212–219, 2022, doi: 10.1016/J.JMRT.2022.09.025.
- [8] A. Andoko, F. Gapsari, I. Wijatmiko, K. Diharjo, S. M. Rangappa, and S. Siengchin "Performance of carbon fiber (CF)/*Ceiba petandra* fiber (CPF) reinforced hybrid polymer composites for lightweight high-performance applications," *Journal of Material Research and Technology*, vol. 27, pp. 7636–7644, 2023, doi: 10.1016/J.JMRT.2023.11.103.



- [9] M. Küçük and Y. Korkmaz, "The effect of physical parameters on sound absorption properties of natural fiber mixed nonwoven composites," *Textile Research Journal*, vol. 82, no. 20, 2012, doi: 10.1177/0040517512441987.
- [10] A. Zent and J. T. Long "Automotive sound absorbing material survey results," *SAE Technical Paper*, 2007, doi: 10.4271/2007-01-2186.
- [11] T. Koizumi, N. Tsujiuchi, and A. Adachi, "The development of sound absorbing materials using natural bamboo fibers," *WIT Transactions on The Built Environment*, vol. 59, pp. 157–166, 2002.
- [12] Z. Sági, R. Butler, and A. Rhead, "Filler materials in composite out-of-plane joints – A review," *Composite Structures*, vol. 207, pp. 787–800, 2019, doi: 10.1016/j.compstruct.2018.09.102.
- [13] M. R. Sanjay, S. Siengchin, J. Parameswaranpillai, M. Jawaid, C. I. Pruncu, and A. Khan, "A comprehensive review of techniques for natural fibers as reinforcement in composites: Preparation, processing and characterization," *Carbohydrate Polymers*, vol. 207, pp. 108–121, 2019, doi: 10.1016/j.carbpol.2018.11.083.
- [14] A. Saravanakumaar, A. Senthilkumar, S. S. Saravanakumar, M. R. Sanjay, and A. Khan, "Impact of alkali treatment on physico-chemical, thermal, structural and tensile properties of Carica papaya bark fibers," *International Journal of Polymer Analysis and Characterization*, vol. 23, pp. 529–536, 2018, doi: 10.1080/1023666X.2018.1501931.
- [15] K. Oksman, A. P. Mathew, R. Långström, B. Nyström, and K. Joseph, "The influence of fibre microstructure on fibre breakage and mechanical properties of natural fibre reinforced polypropylene," *Composite Science and Technology*, vol. 69, pp. 1847–1853, 2009, doi: 10.1016/j.compscitech.2009.03.020.
- [16] D. M. Krishnudu, D. Sreeramulu, and P. V. Reddy, "Optimization the mechanical properties of coir-luffa cylindrica filled hybrid composites by using Taguchi method," *AIP Conference Proceedings*, 2018, Art. no. 020058, doi: 10.1063/1.5032020.
- [17] C. A. Adeyanju, S. Ogunniyi, J. O. Ighalo, A. G. Adeniyi, and S. A. Abdulkareem, "A review on Luffa fibres and their polymer composites," *Journal of Material Science*, vol. 56, pp. 2797–2813, 2021, doi: 10.1007/s10853-020-05432-6/metrics.
- [18] T. Murugan and B. S. Kumar, "Studies on influence of reinforcement characteristics on mechanical properties of banana fiber nonwoven composite structures," in *ICAMR 2019*, pp. 219–231, 2021, doi: 10.1007/978-981-15-8319-3\_24.
- [19] J. C. Posada, L. Y. Jaramillo, E. M. Cadena, and L. A. García, "Bio-based composites from agricultural wastes: Polylactic acid and bamboo *Guadua angustifolia*," *Journal of Composite Materials*, vol. 50, pp. 3229–3237, 2016, doi: 10.1177/0021998315616274.
- [20] B. S. Kumar, T. Murugan, and S. Sakthivel, "Investigation of flexural and dynamic mechanical properties of bagasse fibre composite," *The Journal of the Textile Institute*, vol. 113, no. 12, pp. 2634–2640, 2022, doi: 10.1080/00405000.2021.2001953.
- [21] M. V. Maheshwaran, N. R. J. Hyness, P. Senthamaraiannan, S. S. Saravanakumar, and M. R. Sanjay, "Characterization of natural cellulosic fiber from *Epipremnum aureum* stem," *Journal of Natural Fibers*, vol. 15, pp. 789–798, 2018, doi: 10.1080/15440478.2017.1364205.
- [22] T. Yang, F. Saati, K. V. Horoshenkov, X. Xiong, K. Yang, R. Mishra, S. Marburg, and J. Militký, "Study on the sound absorption behavior of multi-component polyester nonwovens: Experimental and numerical methods," *Textile Research Journal*, vol. 89, pp. 3342–3361, 2018, doi: 10.1177/0040517518811940.
- [23] T. G. Y.s Gowda, M. R. Sanjay, K. Subrahmanya Bhat, P. Madhu, P. Senthamaraiannan, and B. Yogesha, "Polymer matrix-natural fiber composites: An overview," *Cogent Engineering*, vol. 5, 2018, Art. no. 1446667, doi: 10.1080/23311916.2018.1446667.
- [24] S. Boominathan, M. Bhuvaneshwari, K. Sangeetha, K. M. Pachiyappan, and E. Devaki, "Influence of fiber blending on thermal and acoustic properties of nonwoven material," *Journal of Natural Fibers*, vol. 19, no. 15, pp. 11193–11203, 2022, doi: 10.1080/15440478.2021.2021123.
- [25] G. Thilagavathi, E. Pradeep, T. Kannaian, and L. Sasikala, "Development of natural fiber nonwovens for application as car interiors for noise control," *Journal of Industrial Textiles*, vol. 39, pp. 267–278, 2010, doi: 10.1177/1528083709347124.
- [26] A. Ashori, "Wood-plastic composites as promising green-composites for automotive industries," *Bioresource Technology*, vol. 99, no. 11, pp. 4661–



- 4667, 2008, doi: 10.1016/j.biortech.2007.09.043.
- [27] O. M. Abioye, D. A. Olasehinde, and T. Abadunmi, "The role of biofertilizers in sustainable agriculture: An eco-friendly alternative to conventional chemical fertilizers," *Applied Science and Engineering Progress*, vol. 17, no. 1, 2024, Art. no. 6883, doi: 10.14416/j.asep.2023.07.001.
- [28] G. A. Hassan, G. Goud, K. Sathynarayana, and M. Puttegowda, "Influence of water absorption on mechanical and morphological behaviour of Roystonea-Regia/banana hybrid polyester composites," *Applied Science and Engineering Progress*, vol. 17, no. 1, 2024, Art. no. 7074, doi: 10.14416/j.asep.2023.10.003.